JOURNAL OF APPLIED ELECTROCHEMISTRY 21 (1991) 1047–1057

Use of electrochemical techniques to study natural convection heat and mass transfer*

A. A. WRAGG

School of Engineering, University of Exeter, North Park Road, Exeter, EX4 4QF, Great Britian

Received 1 February 1991; revised 19 April 1991

This paper is specifically concerned with the application of the electrochemical limiting current technique to the study of mass transfer and heat transfer by natural convection. A variety of geometries are considered including upward facing discs, inclined plates, cones, cylinders, cuboids and cavities. The case of natural convection due to simultaneous concentration and thermal effects is also considered. A particular feature of the work described is the use of Schlieren photography to obtain flow pattern information. This allows the mass/heat transfer behaviour to be better understood in the light of hydrodynamic observations.

Nomenclature

c_p	specific heat capacity
D	diffusivity
g	gravitational acceleration
Gr	Grashof number ($g\Delta\rho L^3/\nu^2\rho_i$)
GR	combined Grashof number (Equation 5)
H	cuboid aspect ratio
k	mass transfer coefficient
k'	thermal conductivity
L	characteristic length
Sc	Schmidt number ($\mu/\rho D$)
Sh	Sherwood number (kL/D)
Pr	Prandtl number ($c_p\mu/k'$)
Ra	Rayleigh number ($GrSc$ or $GrPr$)
V	cuboid aspect ratio

Greek letters

ν	kinematic viscosity
μ	dynamic viscosity
ρ	density
$\Delta\rho$	density difference

Subscripts

d	diameter
i	interface
m	mass
h	heat
o	stagnant condition
w	based on cuboid width
x	distance
∞	bulk

1. Introduction

This contribution to the series of papers from the Prague Electrodiffusion Flow Diagnostics Workshop is unique in dealing specifically with the question of natural convection occuring at electrode surfaces. Natural convection in electrochemical systems may occur due to species concentration differences in the vicinity of electrodes resulting in density gradients and consequent buoyancy driven flows. These effects may also be complicated by the additional effect of temperature gradients in the vicinity of a working electrode. In cathodic electrodeposition processes the resultant free convection flow due to concentration differences is upwards whereas in anodic dissolution processes, such as electropolishing, the flow is downward.

The paper ranges over a number of applications of the electrochemical limiting diffusion current technique which, in several instances, have been combined with an optical technique. Schlieren photography, in order to gain insight into the hydrodynamic events associated with the mass transfer rates observed. While the present work is centred on the measurement of mass transfer a previous article has drawn attention to the usefulness of the technique in simulating natural convection heat transfer problems [1]. A particular emphasis of the work is the fact that small scale electrochemical measurements can be used to simulate larger scale thermal phenomena due to the very different property numbers, Sc and Pr of the mass and heat transfer processes, respectively.

In most of the situations explored the experimental data have been obtained using copper deposition from acidified copper [2] sulphate solutions at copper or brass cathodes.

The paper is basically subdivided according to the families of geometry considered and is strongly oriented towards flow visualization.

2. Natural convection at horizontal surfaces

Figure 1 provides immediate insight into the vastly different scale of the free convective structure in liquid phase heat transfer and electrolytic mass transfer. The photographs show convection rising from an upward

* This paper was presented at the Workshop on Electrodiffusion Flow Diagnostics, CHISA, Prague, August 1990.

0021-891X/91 $03.00 + .12

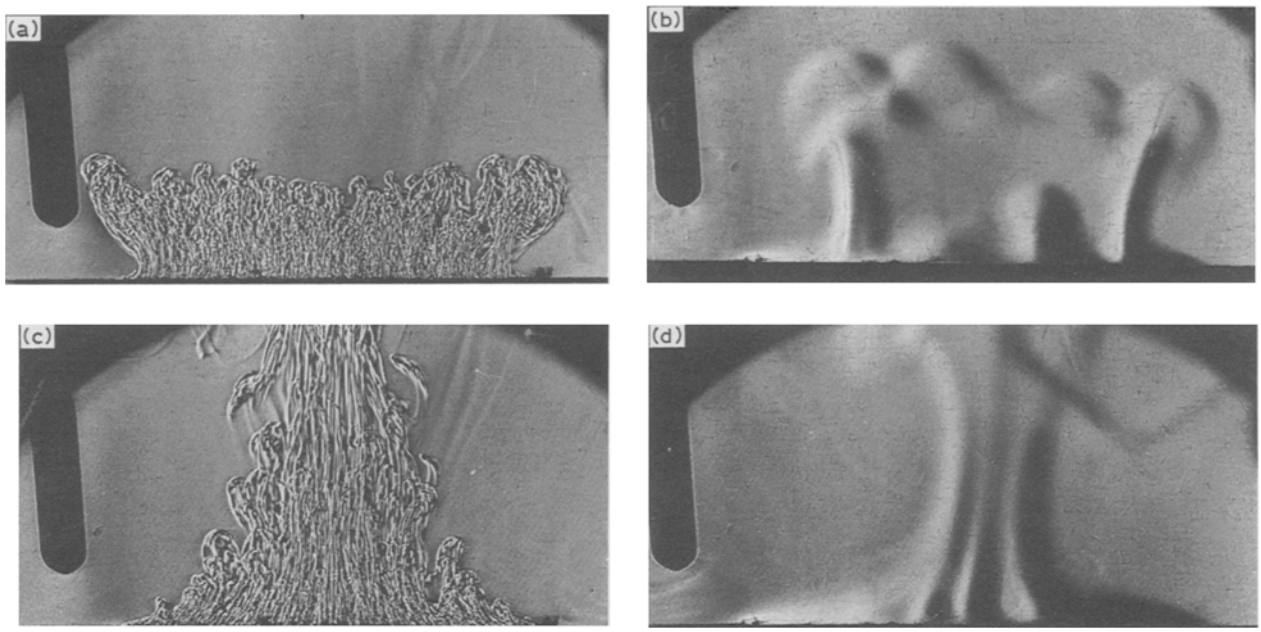

Fig. 1. Contrasting flow structure between electrolytic mass transfer (a and c) and liquid phase heat transfer (b and d) at horizontal up facing discs. Transient experiments. Times after switch-on: (a) 20 s, (c) 45 s, (b) 45 s, (d) 65 s, $Gr_m = 4.86 \times 10^6$, $Gr_h = 1.26 \times 10^6$.

facing isothermal horizontal disc electrode (a) and (c) of diameter 50 mm in copper deposition and from an identically sized electrically heated copper disc (b) and (d). In both cases the development of the convection is being studied using a transient, sudden switch-on technique [2]. The classical thermals in (b) and (d) are coarse in structure and few in number compared to the fine structured convection streams of the mass transfer case. In both cases the Grashof number, based on cylinder diameter is of order 10^6 [3]. This dissimilarity in the scale of the convection suggests that large scale heat transfer situations, especially in gases, where the Prandtl number is lower, can be modelled on small electrode surfaces [1]. In studies focussing on the onset of natural convection at horizontal up-facing surfaces we synchronized the current transient ensuing from a step onset of limiting potential with Schlieren photographs showing stages in the development of the flow. One such sequence is shown as Fig. 2 for a 10 mm diameter electrode in 0.1 M $CuSO_4$ ($Ra = 2.16 \times 10^8$). The diffusion transient ends with the onset of convection; a pulse in the current is associated with the first strong convective surge before steady conditions evolve.

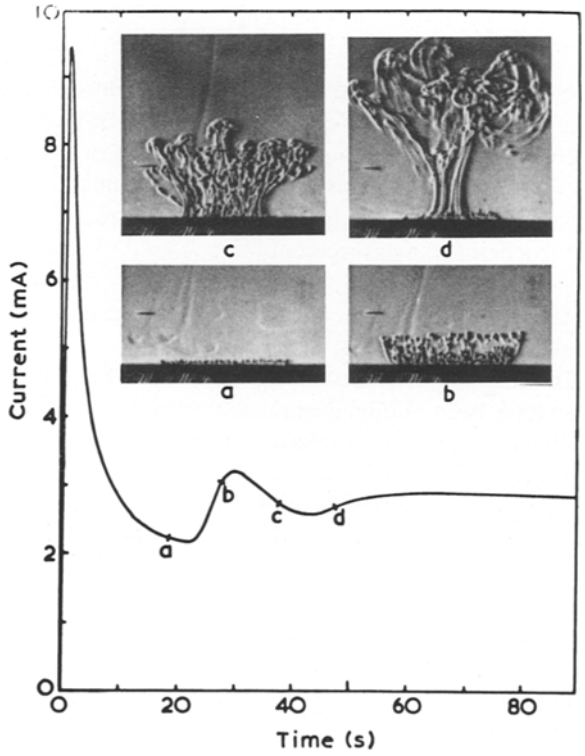

Fig. 2. Current-time transient and associated flow patterns for an upward facing horizontal disc electrode (diameter 10 mm 0.1 M $CuSO_4$).

In some circumstances, notably at electrodes of small diameter, a steady state is not achieved, rather a continuous pulsing flow is maintained as illustrated in Fig. 3a for a 2.5 mm electrode in 0.3 M $CuSO_4$. It can be seen that the current fluctuates with the same frequency as the hydrodynamic pulses, Fig. 3c. This situation stands in marked contrast with the single, steady, laminar plume behaviour of a 1 mm electrode with lower Grashof number (Fig. 3b). An attempt both to correlate mass transfer data and assign the flow regimes resulted in Fig. 4 [2].

A particular problematic aspect of using a metal deposition process in limiting current work is illustrated by Fig. 5 where severe electrode roughening was allowed to take place during an extended (37 min) experiment in 0.3 M $CuSO_4$. The current has increased from the correct steady state natural convection value of 0.68 mA to over 3 mA during this period. This illustrates how metal deposition experiments must be kept as short as possible, and use dilute electrolyte, to avoid the roughening problem. It is of interest to note here how the current changes to an oscillating nature as roughening progresses: this again being reflected in the pulses visible on the rising plumes above the electrode.

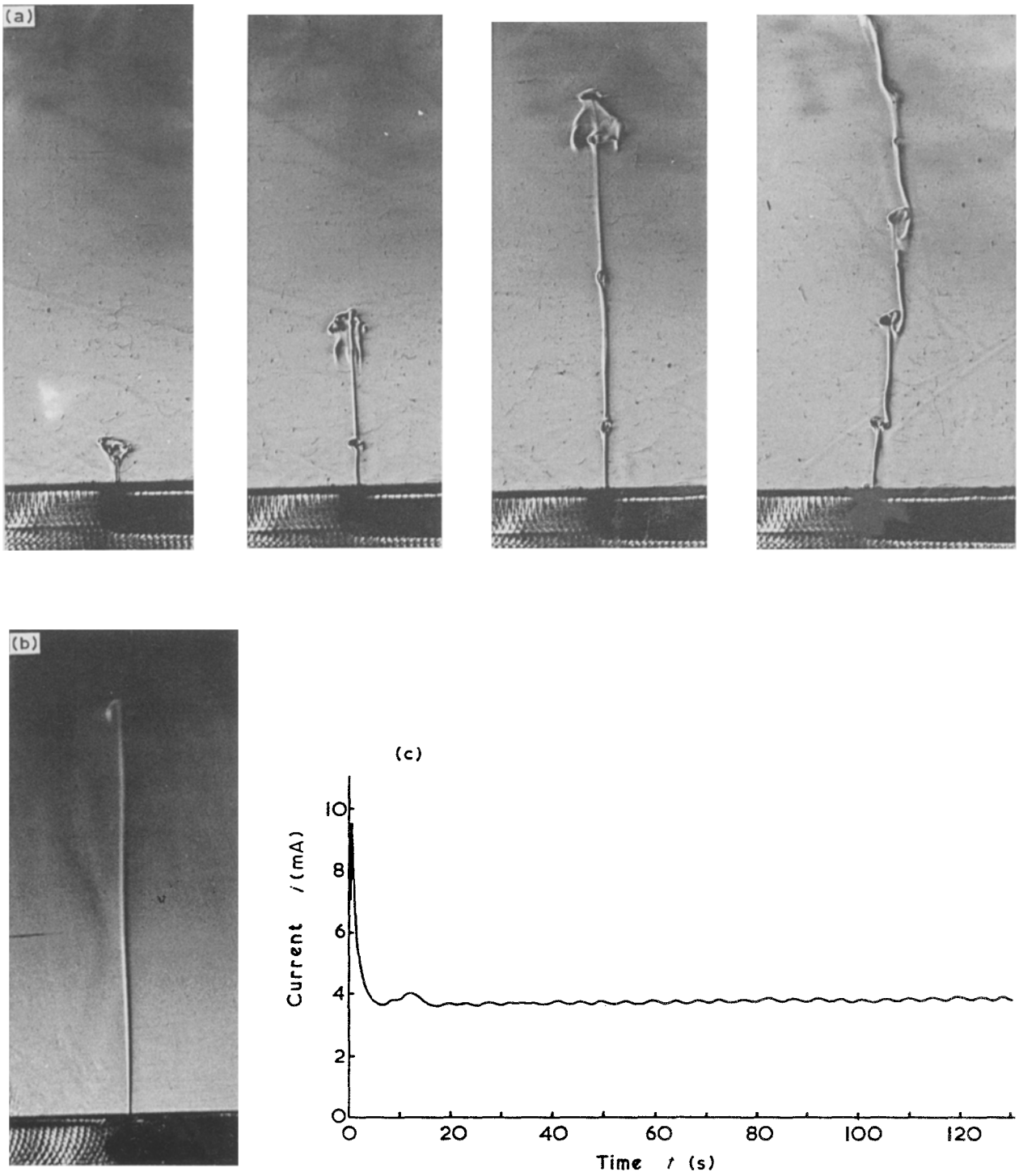

Fig. 3. Plumes showing pulsing (a) or laminar (b) behaviour above small diameter horizontal up-facing disc electrodes: (a) diameter 2.5 mm, (b) diameter 1 mm, (c) current time trace showing a sustained oscillation for the mass transfer rate.

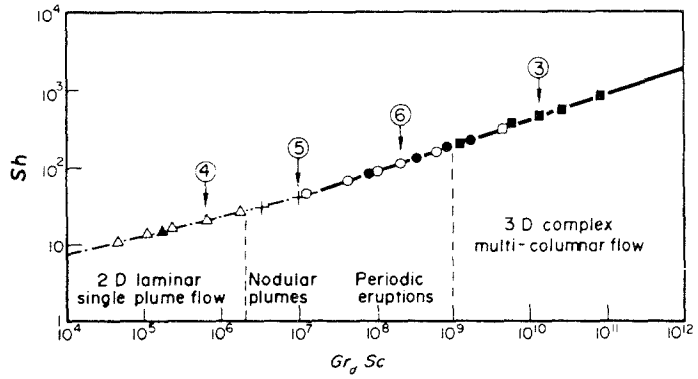

Fig. 4. Correlation of mass transfer data for upward facing horizontal disc electrodes. (△, ▲) Laminar plume, d = 2.5 mm; (+) nodular plume, d = 2.5 mm; (○, ●) periodic eruptions, d = 10.20 mm; (□, ■) multiple eruptions, d = 20.50 mm.

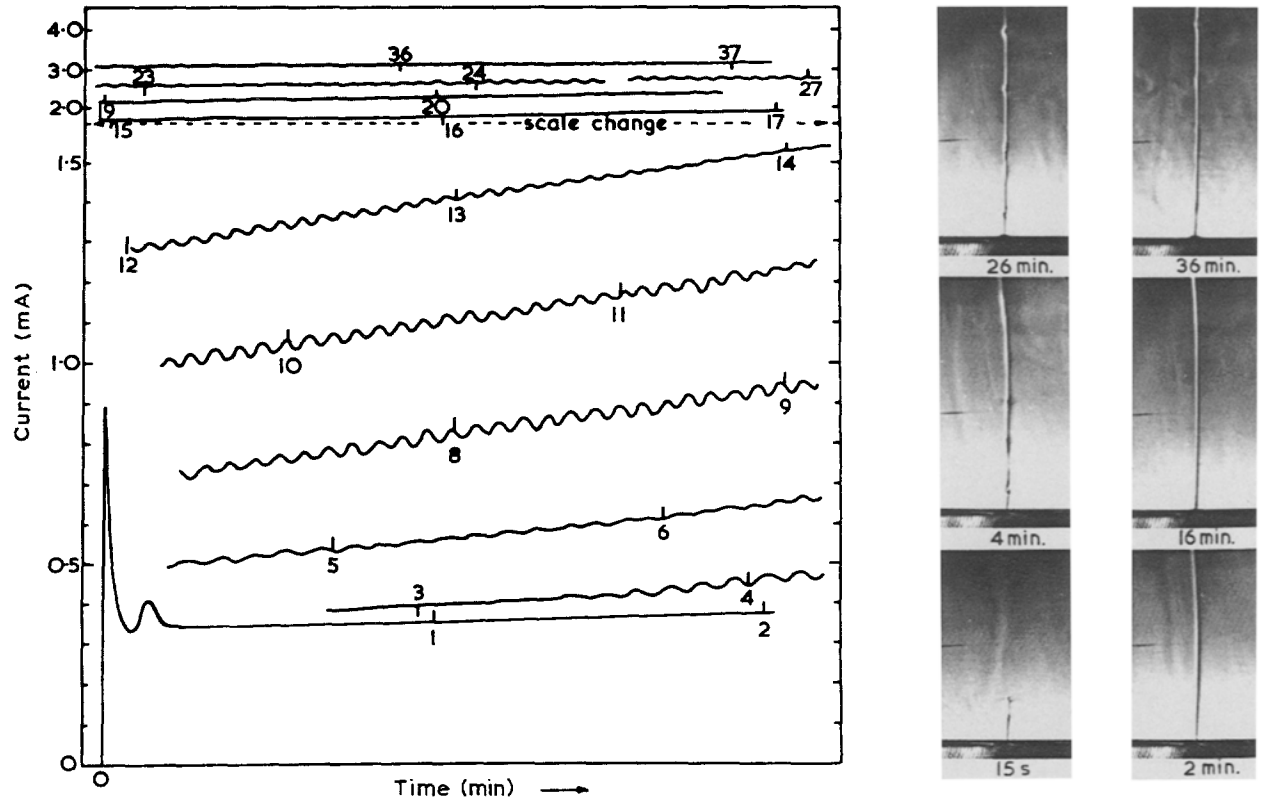

Fig. 5. Current time plot and associated flow visualization for a 1 mm electrode in 0.3 M $CuSO_4$ solution showing long term effects of electrode roughening.

The problem of natural convection in a small gap between two horizontal surfaces is illustrated in Fig. 6 where the copper deposit on the upward facing cathode disc is seen to have a cellular structure corresponding to the flow pattern in the space between the electrodes [4]. The flow situation here approximates to the classical Benard convection obtained in heat transfer in a shallow fluid layer heated from below where regular hexagonal flow cells are produced.

3. Natural convection at inclined surfaces

A thorough study of natural convection at inclined electrodes was made earlier in these laboratories [5] and Fig. 7 provides additional flow visualization for the situation of inclined up-facing plates. Figure 7a clearly shows the boundary layer flowing up the plate and staying attached and laminar. However, as the inclination angle increases (b–d) the flow becomes

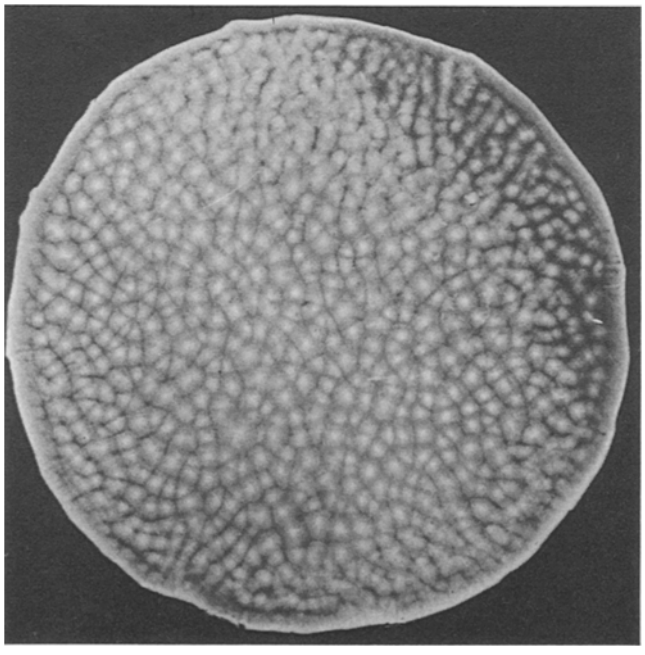

Fig. 6. Electrodeposit on up facing 40 mm copper disc in 0.02 M $CuSO_4$/1.5 M H_2SO_4. Anode-cathode separation was 0.54 mm.

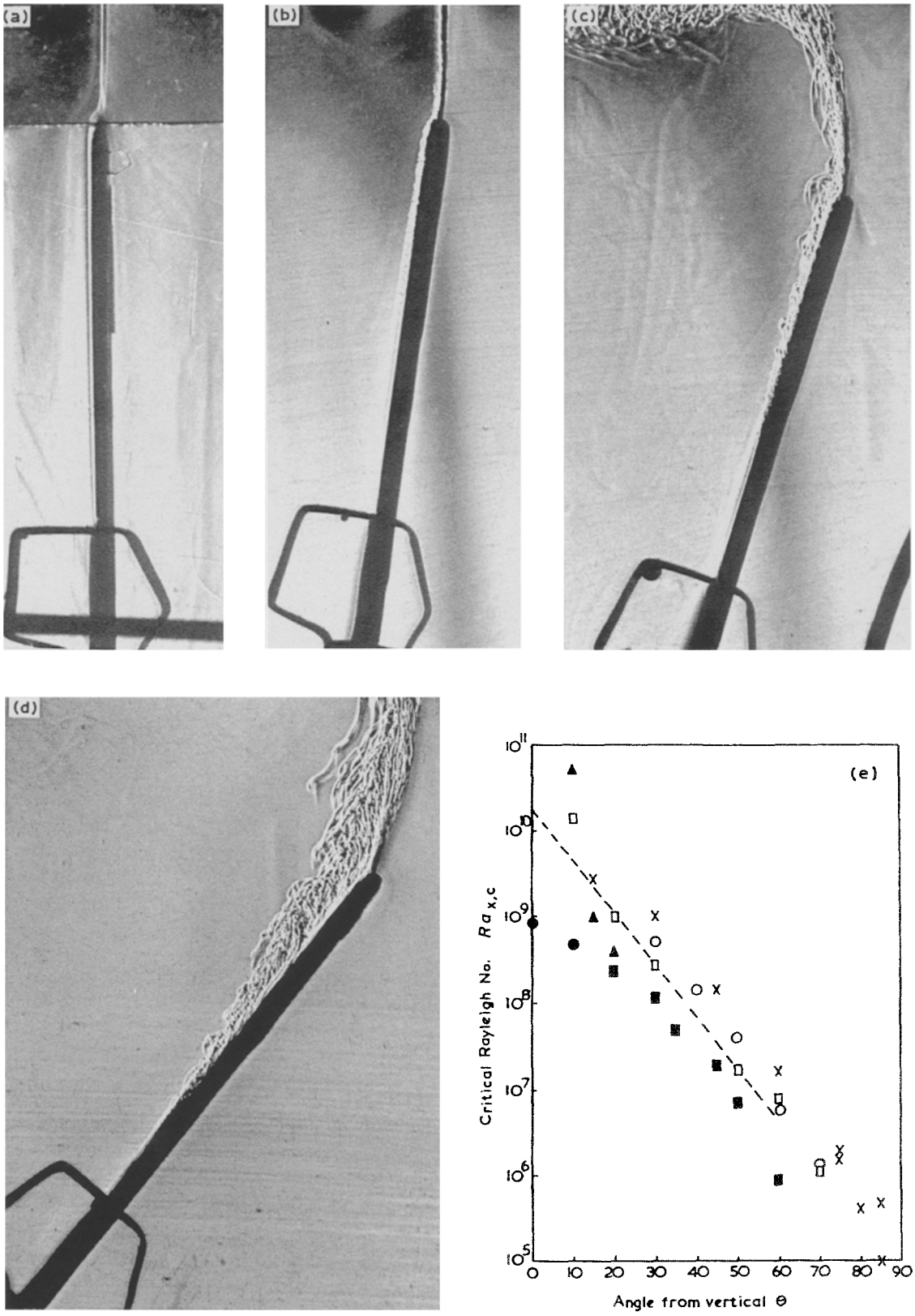

Fig. 7. Flow visualization and instability criteria for natural convection in the $CuSO_4$ system with plane electrodes at different angles of inclination. (▲) Lloyd, Sparrow, Eckert, (●) Lloyd, Sparrow — waves, (■) Lloyd, Sparrow — vortices, and (x) Fujii, Imura. Present: (○) 0.025 and (□) 0.18 M; (— — —) Vliet.

unstable and the point of separation of the flow from the plate progresses towards the leading edge. A plot of the critical Rayleigh number based on this separation distance against angle is shown on Fig. 7e and comparison with other data on flow instability in heat and mass transfer by other authors is shown [6–9]. General agreement is evident. Figure 8a shows how the mass transfer rate, expressed here as the Sherwood number based on plate height, varies with inclination angle and plate height. Mass transfer is seen to be minimum in the horizontal down facing orientation and maximum for horizontal up-facing. Figure 8b gives a

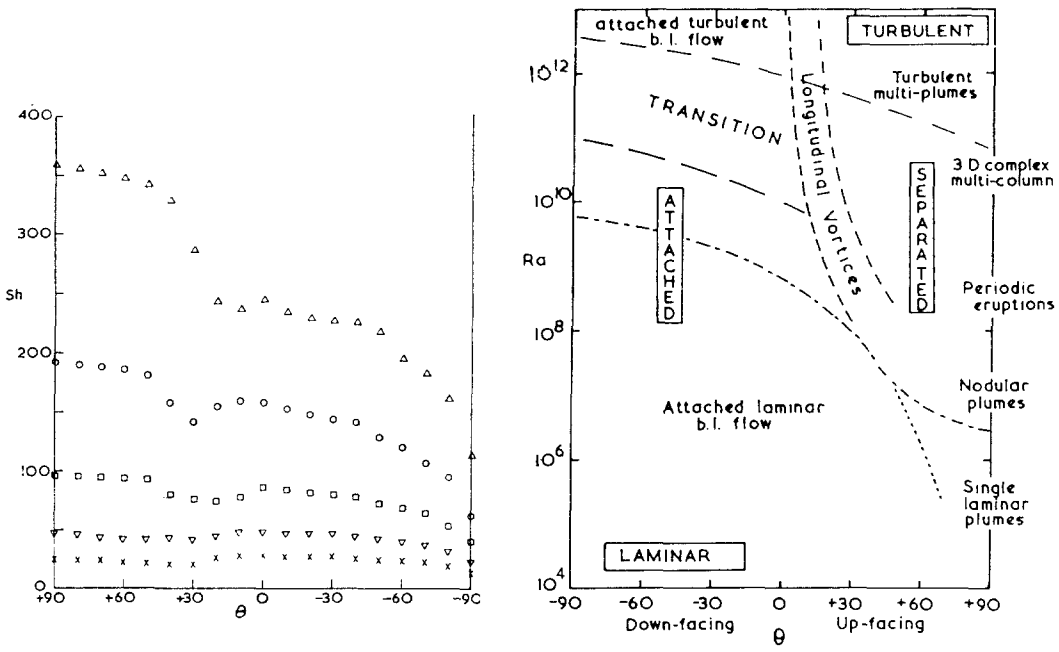

Fig. 8. (a) Variation in Sherwood number with inclination angle for a vertical plate for $C_\infty = 0.04\,\text{mol}\,L^{-1}$; L: (△) 50, (○) 25, (□) 12.5, (▽) 6.2 and (×) 3.1 mm; (b) conjectural flow regime map for natural convection at inclined planes.

conjectural flow regime map [5] which draws attention to the wide variation in flow regimes, which ultimately affect mass and heat transfer rates. All down facing and vertical results were successfully correlated using the equations:

$$Sh = 0.68\,(Gr_\theta Sc)^{0.25} \qquad (1)$$

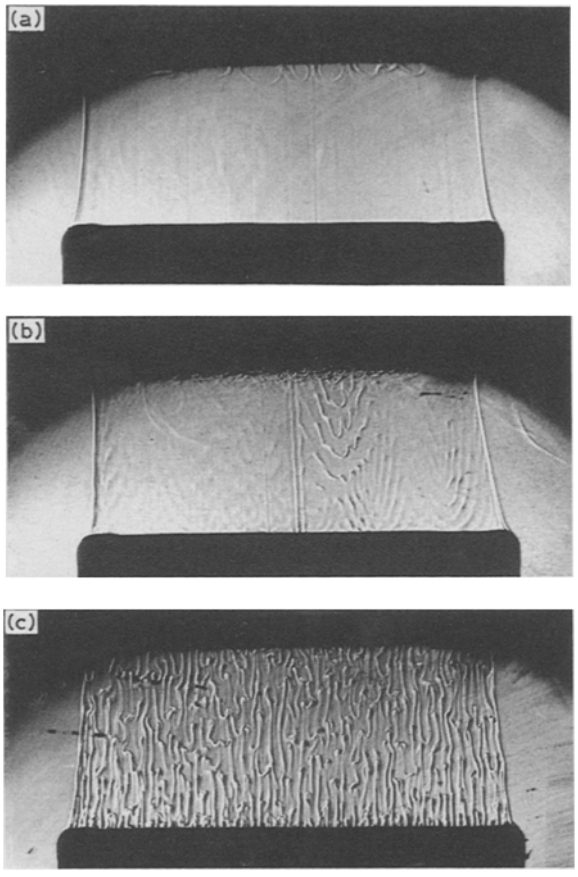

Fig. 9. Schlieren photographs normal to ascending plumes from inclined plate electrodes: (a) vertical plate — no disturbance; (b) 2° from vertical — wave instabilities; and (c) 5° from vertical — longitudinal vortices.

where the Grashof number includes the component of gravitational acceleration parallel to the plate, $g \cos\theta$, the plate height being the characteristic length.

Figure 9 shows Schlieren photographs viewing normal to the plume rising from the top of inclined electrodes. Figure 9a is for a vertical electrode and no disturbance is evident. However, Fig. 9b shows evidence of a wave type instability at an angle of 2° and Fig. 9c shows the well known longitudinal vortices which ascend the plate at slightly higher angles. These vortices produce vertical streaks in the copper deposit, thus illustrating an important link between flow regime and surface effects in electrochemistry.

4. Natural convection at cylinders, cones, cubes and cavities

Figure 10 shows very clearly how flow from one body to another in natural convection can affect the resultant mass transfer rate in entirely different ways. Experiments were performed on single cylinders and vertical arrays of cylinders [10]. Single cylinder data were well correlated by the equation:

$$Sh = 0.56\,(ScGr)^{0.25} \qquad (2)$$

which agreed well with previous work on both heat and mass transfer. Here Fig. 10a shows how flow from the lower cylinder of an array of two impacts on and disturbs the flow at the upper cylinder. The consequent change in the mass transfer rate at the upper cylinder when the lower cylinder is activated results in either a decrease (upper trace) for close-spacing or an increase (lower trace) for a wide spacing.

Flow from an inclined cylinder acting as cathode in copper deposition is shown as Fig. 11. Again the fine structure of the convection streams is evident. Also in such cases the flow around the cylinder (not visible)

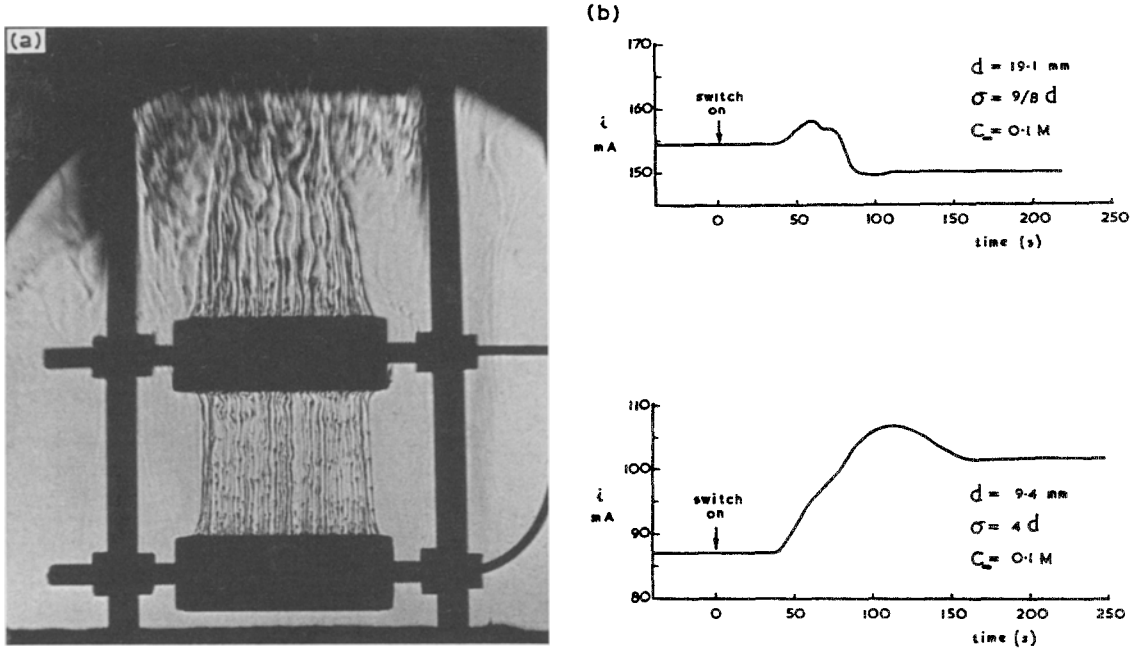

Fig. 10. Natural convection at a vertical array of two horizontal cylinders showing: (a) result of flow from lower cylinder modifying flow at upper cylinder, (b) effect of switch-on of lower cylinder on limiting current at upper cylinder.

tends to ascend spirally and leaves a corresponding spiral impression in the electrodeposit. Work on down facing cone electrodes and double cones has also been carried out in these laboratories [11]. Figure 12 shows convection from a down facing cone where only the down-facing parts are active, the upper horizontal surface being insulated.

Natural convection at vertical and inclined open cavity electrodes was studied by Somerscales and Kassemi [12] and we have also looked at this problem, particularly from the flow visualization aspect [13]. Figure 13 shows flow ascending from an open cavity electrode (sides and base active) of depth 38.1 mm at different times following the switch on of the limiting current potential. The question of how, to satisfy continuity, electrolyte flows into the cavity against the upward buoyancy driven flow is an interesting one. The side to side oscillation of the flow evident in Fig. 13f suggests that this provides a means of fluid ingress to the cavity in the steady state.

In work directed towards the simulation of heat dissipation from electronic components by natural convection we used cuboid electrodes of many different aspect ratios for the measurement of the analagous mass transfer rate [4]. Two examples of the resultant flow field at such electrodes are shown in Fig. 14a and b using the set up shown in Fig. 14c. When considering objects such as cubes (or cuboids) it is necessary to consider the convection at each of the six faces and the possible interactions in the flow. Using this approach we successfully correlated data from a wide range of cuboids and obtained excellent agreement with heat transfer data [14]. Using a 'separate faces' approach and an interaction factor, f, the mass transfer correlating equation in laminar flow from all cuboid electrodes was:

$$Sh_w - Sh_0 = \left\{\frac{f(0.675(1 + H)V^{3/4} - 0.321H) + 0.161H}{H + V + VH}\right\} \times (Ra\, F(Sc))^{0.25} \quad (3)$$

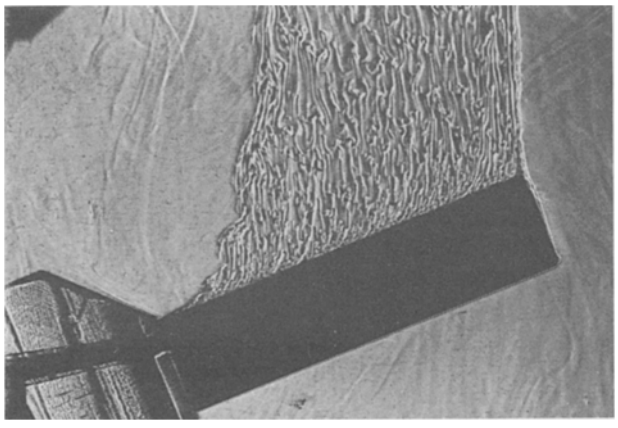

Fig. 11. Natural convection flow at an inclined cylinder electrode.

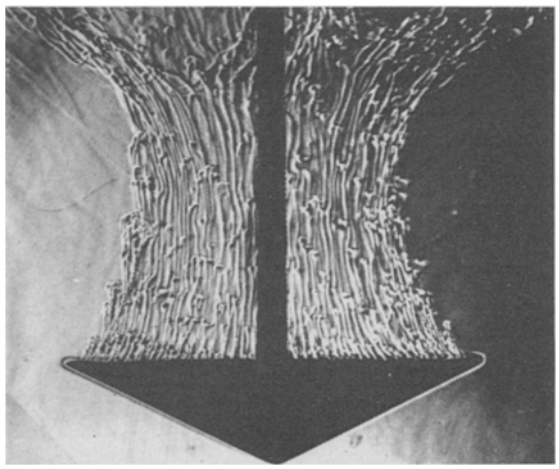

Fig. 12. Natural convection flow from a down facing conical electrode. Upper horizontal surface is insulated ($CuSO_4/H_2SO_4$ system).

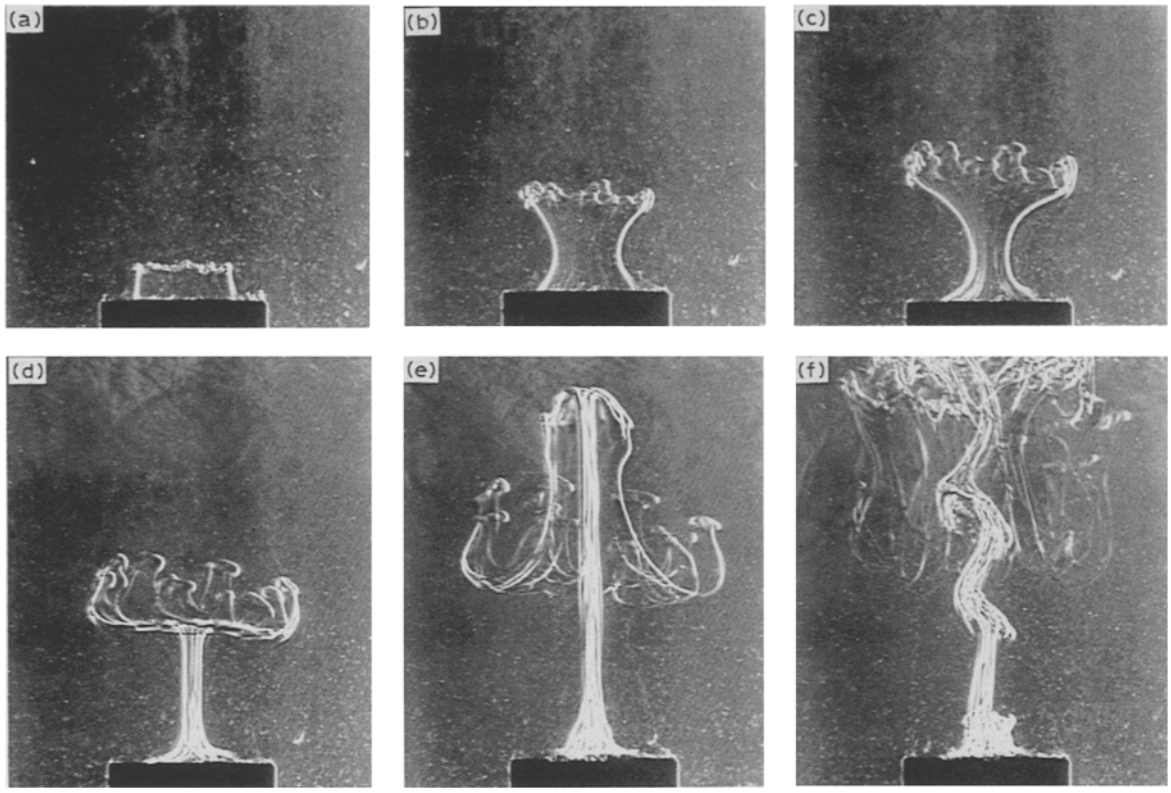

Fig. 13. Flow emerging from an open vertical cavity electrode (diameter 13.5 mm, depth 38.1 mm) in 0.16 M $CuSO_4$. Times after onset of limiting polarization are (a) 14, (b) 22, (c) 26, (d) 31, (e) 41, and (f) 65 s.

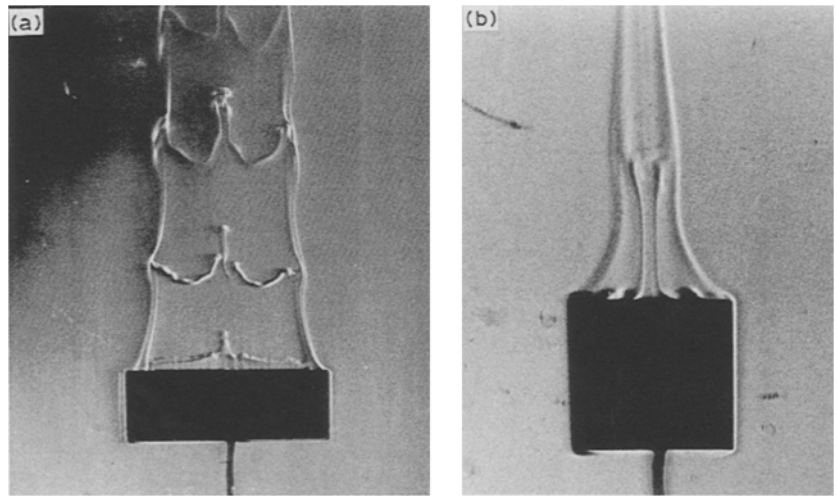

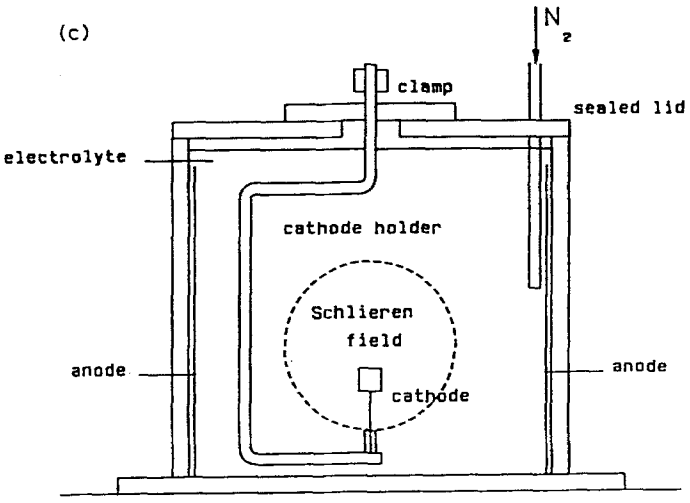

Fig. 14. Convection at cuboid electrodes (a and b) simulating heat transfer at electronic components from the work of Worthington [14] (c) shows the disposition of the electrodes with respect to the Schlieren beam.

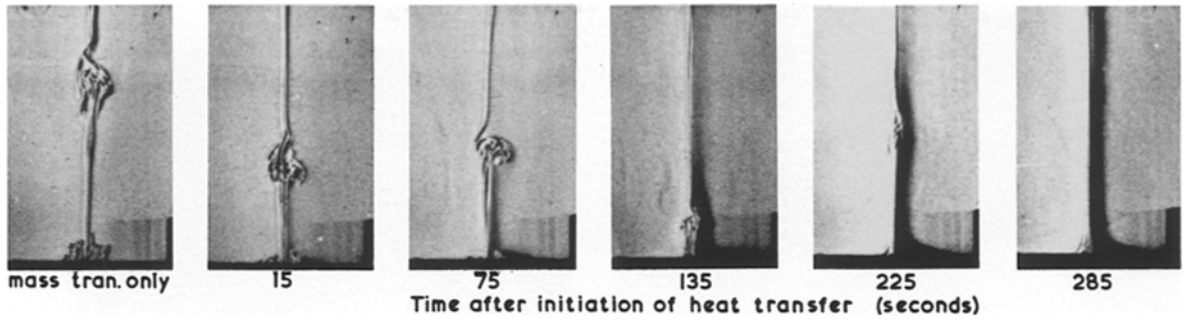

Fig. 15. Effect of progressive implementation of heat transfer on the plume above a horizontal 10 mm diameter electrode. At 285 s $(T_i - T_\infty)$ is 4.0° C. Concentration is 0.03 M $CuSO_4$.

where V and H are cuboid aspect ratios and where

$$F(Sc) = \left(1 + \left(\frac{0.5}{Sc}\right)^{4/16}\right)^{-16/9} \quad (4)$$

5. Natural convection with combined mass and heat transfer

In earlier work on mass transfer at heated up-facing horizontal electrodes [15] we were able to successfully correlate the mass transfer data using a combined Grashof number (GR_m) embodying the concentration (Gr_m) and thermal (Gr_h) Grashof numbers:

$$GR_m = Gr_m + (Sc/Pr)^{1/2}\, Gr_h \quad (5)$$

Flow visualization experiments demonstrated the interaction of the concentration and thermally driven flow fields [3]. Figure 15 shows how the progressive strengthening of thermal convection at a horizontal electrode changes the pulsing nature of the flow (mass transfer only) to a situation involving a single ascending plume.

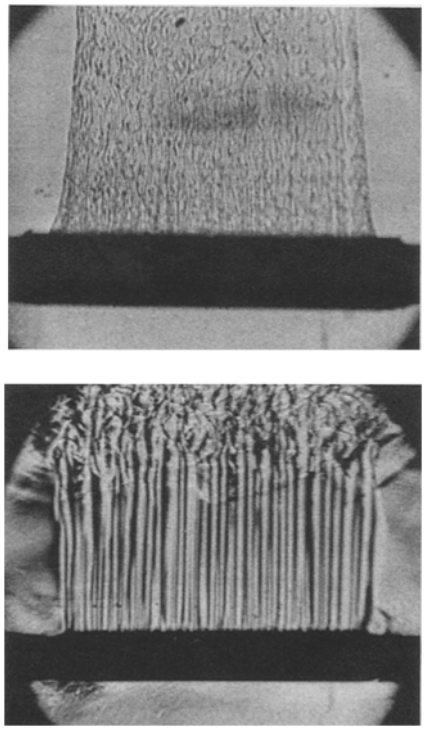

Fig. 16. Comparison of flow structure at horizontal 15 mm diameter cylinder electrodes for (a) an isothermal system, (b) an electrode at 60° C.

More recent work has considered combined convection at horizontal cylinders [16, 17]. The marked change in the length scale of the convective structure between an isothermal (Fig. 16a) and a heated horizontal cylinder (Fig. 16b) is very apparent. Here the heated cylinder surface temperature is 60° C and the bulk electrolyte is maintained at 19° C. Increase in surface temperature has a very pronounced effect on mass transfer coefficient but it has been possible to correlate data from different cylinder diameters, concentrations and surface temperatures using the combined Grashof number defined in Equation 5 as shown in Fig. 17. Here the correlating equations are:

$$Sh = 0.53(GR_m Sc)^{1/4} \quad (6)$$

and

$$Sh = 0.018(GR_m Sc)^{2/5} \quad (7)$$

the transition occurring at a $GR_m Sc$ value of approximately 2×10^9.

6. Natural convection in anodic dissolution

In anodic metal dissolution processes, such as electropolishing, there is a density increase at the electrode/electrolyte interface and a resultant downward flow. Figue 18a shows such convection from a down facing copper disc electrode of diameter 25 mm electro-

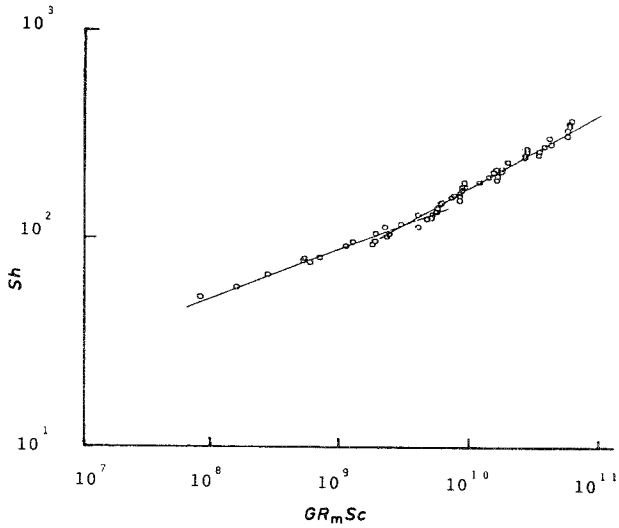

Fig. 17. Correlation of data for combined mass and heat transfer at horizontal cylinder electrodes.

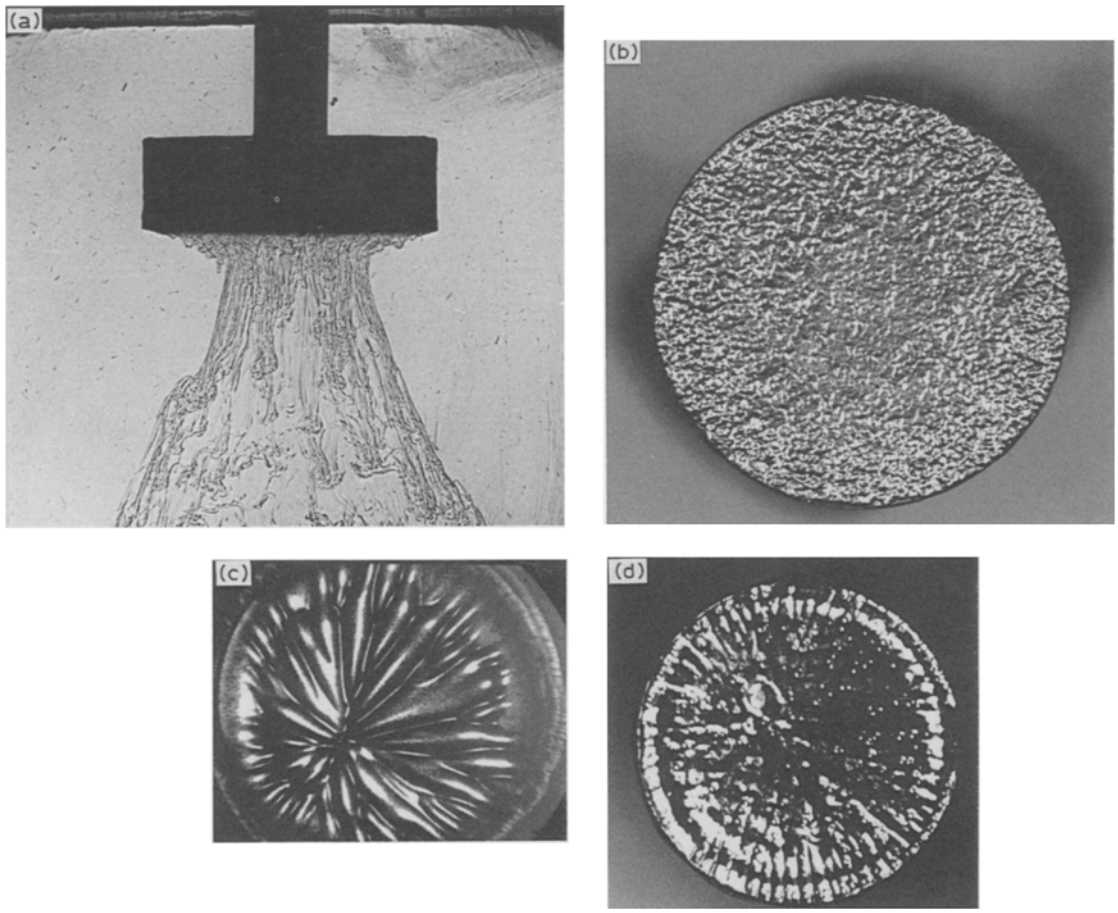

Fig. 18. Flow and surface effects in electropolishing of copper in phosphoric acid medium at down-facing surfaces in natural convection. (a) Downward convection; (b) dimpled polished finish due to multi-plume convection at a large surface; (c) and (d) radial striations in polished surface at smaller electrode diameters.

polishing in orthophosphoric acid medium. Interesting flow effects may be observed on the surfaces of electropolished specimens under natural convection conditions [18]. Figure 18b shows a polished specimen of 50 mm diameter with a bright but dimpled, orange peel-like surface resulting from local convection cells. For smaller diameters the radial inflow, (Fig. 18a) feeding a single plume at a 2.5 mm electrode, leads to radial, converging grooves in the polished surface. The larger 10 mm electrode shown in Fig. 18d again shows radial striations corresponding to rotational inflow near the disc periphery.

7. Conclusions

This paper has sought both to illustrate the combined use of optical and electrochemical techniques to elucidate natural convection flow behaviour and also to demonstrate how surface topography in both electrochemical deposition and dissolution processes may be influenced by the nature of such flows. Unlike in many forced convection flow problems the use of small sensing electrodes has not been used. Indeed the use of such electrodes in natural convection is suspect due to the possibility of triggering discrete and unrepresentative hydrodynamic events. Nonetheless, such studies using the limiting diffusion current technique at macro-electrodes have made a valuable contribution to the understanding of mass transfer, heat transfer and the related fluid flow in a variety of geometries of electrochemical and engineering interest.

Acknowledgements

I am indebted to my colleague Mike Patrick for many years of valued collaboration in this work. Thanks are also due to the following sometime student colleagues who have made contributions in various aspects to the work: Elizabeth Connor, D. H. Worthington, D. M. Thomas, A. K. Nasiruddin, Kok Leong Wong, D. M. Pargeter, A. F. J. Smith, Hanifi Sarac, M. R. Southcoat, T. D. Harding, J. D. Simmons, A. D. S. Norton and L. H. Mustoe.

References

[1] M. A. Patrick and A. A. Wragg, *I. Chem. E. Symposium Series* No. 94 (1985) 45.
[2] *Idem, Int. J. Heat Mass Transfer* **18** (1975) 1397.
[3] *Idem, Electrochim. Acta* **19** (1974) 929.
[4] K. L. Wong, University of Exeter, Unpublished Work (1985).
[5] M. A. Patrick, A. A. Wragg and D. M. Pargeter, *Canadian J. Chem. Eng.* **55** (1977) 432.
[6] J. R. Lloyd, E. M. Sparrow and E. R. G. Eckert, *Int. J. Heat Mass Transfer* **45** (1972) 457.
[7] J. R. Lloyd and E. M. Sparrow, *J. Fluid Mech.* **42** (1970) 564.

[8] T. Fujii and H. Imura, *Int. J. Heat Mass Transfer* **15** (1972) 755.
[9] G. C. Vliet, *J. Heat Transfer* **91** (1969) 511.
[10] A. F. J. Smith and A. A. Wragg, *J. Appl. Electrochem.* **4** (1974) 219.
[11] M. A. Patrick and A. A. Wragg, *Physicochem. Hydrodynamics* **5** (1984) 299.
[12] E. F. C. Somerscales and M. Kassemi, *J. Appl. Electrochem.* **15** (1985) 405.
[13] D. A. Thomas, University of Exeter, Unpublished work (1987).
[14] D. H. Worthington, M. A. Patrick and A. A. Wragg, *Chem. Eng. Res. and Desn.* **65** (1987) 131.
[15] A. A. Wragg and A. K. Nasiruddin, *Electrochim. Acta.* **18** (1973) 619.
[16] A. A. Wragg, H. Sarac and M. A. Patrick, Extended Abstracts, IX Congress Iberoamericano de Electroquimica, La Laguna (July 1990) 712.
[17] H. Sarac, A. A. Wragg and M. A. Patrick, submitted to *Int. Commun. Heat and Mass Transfer*.
[18] A. A. Wragg, M. A. Patrick, S. J. Ashcroft and Elizabeth Connor, Extended Abstracts 32nd ISE Meeting, Cavtat, Yugoslavia (1981).